Journal of Glaciology, Vol. 34, No. 117, 1988

SNOW-SLOPE STABILITY – A PROBABILISTIC APPROACH

By H. CONWAY* *and* J. ABRAHAMSON

(Department of Chemical and Process Engineering, University of Canterbury, Christchurch, New Zealand)

ABSTRACT. Measurements of snow properties across and down snow slopes have been used to calculate a safety margin — the difference between the basal shear strength and the applied static stress. Areas of basal deficit exist when the applied shear stress exceeds the basal shear strength (the safety margin is negative), and basal areas are pinned when the safety margin is positive. As the size of deficit increases, stresses within the overlying slab also increase, and these may be sufficient to cause an avalanche.

Measurements made on five slopes (four of which had avalanched) were characterized by considerable spatial variability, and the safety margin has been treated as a random function which varies over the slope. Statistical models of Vanmarcke (1977[a], 1983) have been applied to determine the most likely size of deficit required for avalanching (95% confidence). In one case, an avalanche occurred when the length of deficit was only 2.9 m, and in the other cases the length was always less than 7 m. This size of deficit is small compared with the total area of many avalanche slopes which suggests that avalanches initiate from small zones of deficit, and makes it difficult to locate a deficit with just a few tests.

The optimum sampling interval and number of tests required to yield an adequate estimate of the statistical parameters of the safety margin are also discussed.

INTRODUCTION

Because we can hope to make only a few measurements of snow strength and stress over any particular slope, we need to estimate the continuous spatially varying properties from a finite number of "point" measurements. Furthermore, we would like to minimize the number of measurements required to represent adequately a slope. Several techniques have been used to extrapolate properties over large areas from just a few measurements (e.g. Kriging — see Krige, 1966; or Monte Carlo simulations — see Harr, 1977, 503-54; or Nguyen and Chowdhury, 1985), and we have chosen a technique proposed by Vanmarcke (1977[a], 1983).

A series of contiguous point measurements made at intervals over a slope may be treated as a "stationary random process". Such a process can be characterized by a mean value, a variance or standard deviation, and a measure of the influence between adjacent measurements. The influence (or correlation structure) of a random process is commonly represented either by a correlation function or by a Fourier transform, but Vanmarcke (1977[a], [b], 1983) has proposed a new approach using a "moving average" technique. A small amount of local averaging is allowed and this serves to smooth micro-scale fluctuations which can give rise to excessive sensitivity. Adjacent measurements are averaged to generate a locally averaged random function with a changed variance. The averaging procedure can be extended over larger lengths to produce a family of functions.

As an example of the extended averaging procedure, measurements of basal shear strength (taken from case 2 discussed below) have been averaged and plotted in Figure 1a. The figure shows the original "point" measurements and also the measurements averaged over 2.67 and 6.23 m. As the averaging length is increased, fluctuations about the mean tend to cancel, causing the variance to diminish. The manner in which the variance diminishes is a reflection of the correlation between adjacent measurements, and a variance function is defined as the ratio of the variance of the locally averaged process to the variance of the original point process. For the example shown in Figure 1a, the variance function is:

$$\Gamma^2 = \frac{\text{var } \sigma_{bL}}{\text{var } \sigma_{bo}} \qquad (1)$$

where var σ_{bo} and var σ_{bL} are respectively the variance of point measurements of shear strength, and the variance of measurements which have been averaged over length L. This function (plotted in Figure 1b) fully characterizes the correlation structure of the original process and contains the same information as a correlation function or a spectral density function.

The decay in variance can be described in terms of a "scale of fluctuation", δ, which defines the scale at which increased averaging commences to have a significant influence on the variance. Numerous specific analytical models of the variance function can be used, and one of the simplest takes the form:

$$\begin{aligned} \Gamma^2 &= 1 && \text{for } L \leqslant \delta, \\ &= \delta/L && \text{for } L > \delta. \end{aligned} \qquad (2)$$

This function provides a reasonable approximation of the variance function, especially when the averaging length exceeds about 2δ, and is also plotted for the example in Figure 1b.

Random processes for which $\delta \to 0$ have no long-term memory, and under extended local averaging the variance decay is in inverse proportion to L^2 (rather than L). This further simplifies calculations because values can be assumed to be independent. However, any random process may be sufficiently described by a mean, variance, and scale of fluctuation, making for simple derivations of the mean-square derivative, mean threshold-crossing rates, and the probability distribution of extreme values.

Physically, there exists an approximate relationship between δ and the average length the point process is above (or below) its mean value. In fact, the half wavelength of the process, $\lambda/2$, can be approximated by (Vanmarcke, 1977[a], 1983):

$$\lambda/2 = (\pi/2)^{1/2}\,\delta \qquad (3)$$

$$= 1.25\delta.$$

* Present address: Geophysics Program AK-50, University of Washington, Seattle, Washington 98195, U.S.A.

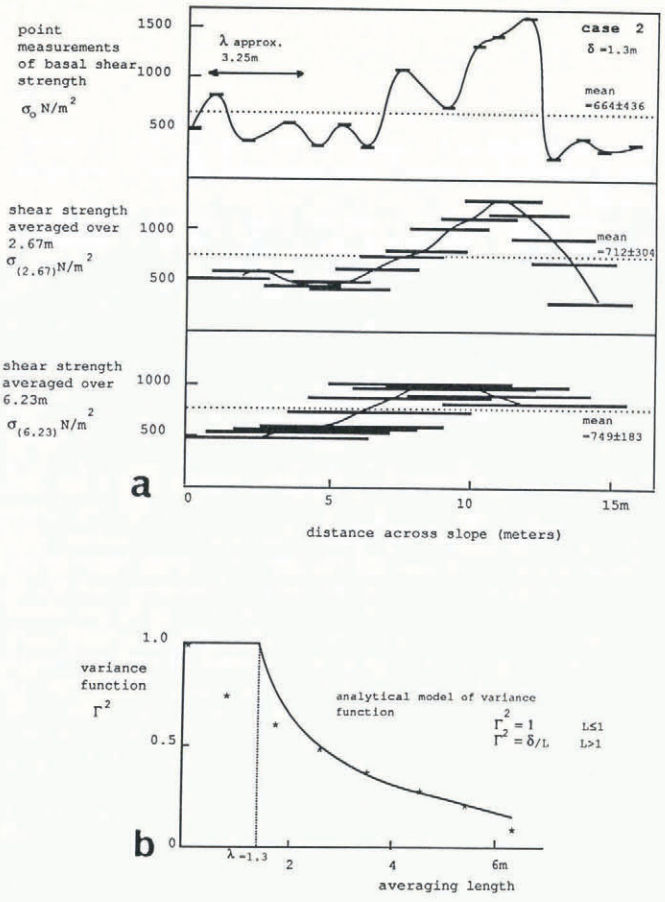

Fig. 1a. An example of how extended local averaging of point measurements of a property can be used to generate a family of random processes. The upper plot shows "point" measurements of basal shear strength (taken from case 2). These were measured over an area of about 0.1 m² and spaced 0.89 m apart, and were measured across the slope. The lower plots show the point measurements averaged over 2.67 and 6.23 m. With increased averaging, the variance of successive functions diminishes.
*b. For the same example (case 2), the lower plot shows how the ratio of the variance of the averaged values to the variance of the original point values can be used to construct a variance function (marked by *). The variance function can be approximated by an analytical model (solid curve) to calculate a scale of fluctuation. For the basal shear-strength measurements shown, δ = 1.3 m.*

Risk of local failure

A potential slab avalanche can be described as a relatively stiff slab of snow overlying a weak layer (or weak interface between layers). We define the difference between the resisting basal shear strength (σ_b) and the static driving stress (S_D) as a safety margin (SM), and a "basal shear deficit" to occur when the safety margin is negative. Areas where the safety margin is positive are called "pinned" areas. A deficit will cause the stresses within a slab to increase which may initiate slab-failure processes, particularly in cases where the strength of the slab is small (e.g. in low-density, shallow slabs). In this paper we consider the driving stress to comprise of the gravitational stress (τ_g — determined for the "infinite" slab condition), plus any extra static slope-parallel stress (S_E — such as the weight of a skier or cornice fall, etc.):

$$S_D = \tau_g + S_E = \rho g h \sin\theta + S_E \quad (4)$$

where ρ is the slab density, g is the gravitational acceleration, h is the slab depth, and θ is the bed-surface angle.

The safety margin can be treated as a random process in the manner described above and is:

$$SM = \sigma_b - S_D, \quad (5)$$

and for point locations, the probability of a basal shear deficit is therefore:

$$P_0 = P(SM_0 \leqslant 0) \quad (6)$$

where SM_0 is derived from point measurements of basal strength (σ_{b0}), and driving stress (S_{D0}).

A localized point deficit may not be large enough to affect the stability of a slope, and we are interested in deficits which extend over larger areas. The probability that a deficit will exist over an area A is:

$$P_A = P(SM_A \leqslant 0) \quad (7)$$

where SM_A is derived from measurements which have been averaged over an area A.

If the random functions SM_0 and SM_A can be described by normal distributions, the probability can be represented by a standard normal variate. If $\overline{SM}_A$ is the mean value of the averaged function, and $\widehat{SM}_A$ is the standard deviation, then the standard normal variate B_A is:

$$B_A = \frac{\overline{SM}_A - 0}{\widehat{SM}_A}. \quad (8)$$

The probability of a basal deficit (P_A) can then be obtained by entering probability tables for normal distributions. As the averaging area increases, the distribution becomes more defined ($\widehat{SM}_A$ decreases), and the probability of finding a deficit which spans that area decreases.

Risk of slope (or "system") failure

Equation (7) gives the probability of a deficit of area A at a specific location. For a slope or system failure, we are interested in the probability that a deficit will exist at any location over the whole slope. A convenient way to view this problem is by a "first-crossing" analysis in which crossings of a certain level by the process are considered. In our case, we are interested in a crossing of the zero-stress level by the safety-margin function.

The simplest and commonly used model of this condition is to consider the crossings/no-crossings as a binary random series which is 0 if the safety margin is positive, and 1 if the safety margin is negative. This type of counting process has a binomial probability function and is limited to functions which are not correlated ($\delta \to 0$, and adjacent values are statistically independent). If the probabilities P_A for each specific area of deficit (or "component") are equally likely, then for a total of N components ($N = A_t/A$), the probability that a deficit exists somewhere across a slope of total area A_t is (Harr, 1977):

$$P_{At,A} = 1 - (1 - P_A)^N. \quad (9)$$

If adjacent components are correlated, Equation (9) gives a low estimate of probability and the correlation structure needs to be considered. Rice (1944) derived an expression to describe the expected rate of crossings by a one-dimensional Gaussian random process. The level to be crossed was assumed to be far from the mean value of the function which ensures crossings would be rare and therefore independent, and so a Poisson distribution can be used to describe the crossings. Vanmarcke (1977[a], [b], 1983) applied the moving average approach to Rice's work and, for an averaged Gaussian function, the mean rate of crossings per unit length (ω_L) is:

$$\omega_L = \frac{1}{2\pi}\left[\frac{2}{L\delta}\right]^{\frac{1}{2}} \exp\left(-\frac{B_L^2}{2}\right). \quad (10)$$

This expression describes crossings by a one-dimensional function which has been locally averaged over a length L; B_L is the standard variate of this function, and δ is defined

https://doi.org/10.3189/S0022143000032196 Published online by Cambridge University Press

by Equation (2). Over a total length L_t the probability of one crossing (or first crossing) by an averaged function is:

$$P_{Lt,L} = 1 - (1 - P_L)\exp(-\omega_L L_t) \quad \text{for } L_t > L. \quad (11)$$

P_L is the probability of a local deficit of length L. (For derivation and analysis of the first-crossing results, see Crandall, and others (1966) and Vanmarcke (1975, 1983)).

Extension of Vanmarcke analysis to two dimensions

In order to account for variation and correlation between properties both across and down slopes, a two-dimensional analysis is required. Vanmarcke (1983) showed how the moving-average techniques could be extended to multi-dimensional processes and still remain tractable. For a two-dimensional process, the appropriate variance function can be expressed as the product of two one-dimensional variance functions, each with a scale δ_x and δ_y. If the two one-dimensional functions are separable, for a function averaged over area A, Equation (10) may be rewritten to estimate the mean rate of crossings per unit area:

$$\omega_A = \frac{B_A}{(\pi^3 2A\delta_x\delta_y)^{1/2}}\exp\left(-\frac{B_A^2}{2}\right). \quad (12)$$

For a total slope area of A_t, the probability of a crossing is:

$$P_{At,A} = 1 - (1 - P_A)\exp[-\omega_A A_t] \quad \text{for } A_t > A. \quad (13)$$

P_A is the probability of a local deficit over area A.

It is clear from either Equation (9) or Equation (13) that, for a given probability of a local deficit, the probability over the whole slope will increase with the area of slope.

Clustering of crossings

If the mean value of a random process is close to the level to be crossed, the probability of a single crossing increases, and crossings may not be independent. In these cases, more than one peak may occur during each crossing, causing "clumping" or "clustering" of values and the period the random function spends above (or below) the level increases. Furthermore, the interval between crossings also increases and Vanmarcke (1983) showed how the Poisson distribution could be adapted by using a "mean rate of crossings". In our case, clustering would increase the expected size of deficit, especially when $B_A < 2$.

ANALYSIS OF CASE HISTORIES

Our measurements of basal shear strength (described fully in Conway and Abrahamson (1984)) were made by isolating a column of snow from effects of side shear, compressive and tensile hold-up to a depth greater than the suspected shear plane, and then applying a force to fracture the column. The basal shear strength was taken to be the sum of the gravitational stress and the extra stress required for fracture. Each measurement (or "point" value) was made over an area of about 0.1 m^2 (the area was measured after each test), and the distance between measurements varied from 0.6 to 0.89 m. At each site, as well as estimates of basal shear strength, we measured the bed-surface angle, average slab density, and depth of slab, and a summary of these data is shown in the Appendix.

Measurements had been made on slopes at the head of Tasman Glacier (2130 m) in New Zealand. Of the five sets of data, one (case 1, 19 September 1982) had avalanched naturally about 12 h prior to making the measurements, three (case 2, 13 July 1982; case 3, 1 August 1984; case 4, 28 August 1984) were small avalanches which avalanched only after skiing near the crownwall, and the other (case 5, 1 August 1983) fractured locally after ski-loading, but did not avalanche.

Statistical analysis of measurements

Gubler (1978) suggested a log-normal distribution to describe the strength of force conducting elements within a snow-pack because strength cannot take negative values and also bond and grain diameters in many sintered materials are often characterized by this distribution. However, the safety margin is likely to have a complex probability density function governed by the relative contributions from both the stress and the strength components. To simplify the calculations and because of the Central Limit theorem, we have used a normal distribution to describe the safety margin.

Our method of measuring basal shear strength had definite upper and lower limits. For samples where the down-slope gravitational weight of snow exceeded the basal shear strength, the column failed before extra loading could be applied, and the strength was less than the gravitational weight. In some tests, we could not apply sufficient stress to fracture the sample. In order to use all measurements, including those above and below these stress levels, and still arrive at an unbiased estimate of population mean and variance, we made use of order statistics and "best linear estimate" techniques outlined by Sarhan and Greenberg (1962, p. 206-09). The estimates of population mean and standard deviation are made by multiplying each observation by an appropriate coefficient (tabulated by Sarhan and Greenberg for normal distributions of sample size 20 or less). Teichroew (*in* Sarhan and Greenberg, 1962, p. 190-205) tabled expected values for an ordered normal distribution with a specific mean and standard deviation. We used these tables to obtain the "censored" values (values lying above the upper, and below the lower stress levels), and then used a random-number chart to assign the censored values to a spatial location on the slope. For these slopes, 35 shear measurements (out of a total of 87) were censored values.

The measurements of shear strength are characterized by considerable spatial variability, and case 2 is shown as an example in Figure 1a. Point measurements (including censored values) are plotted in the upper curve, and the lower curves are derived from measurements which have been averaged over 2.67 and 6.23 m. Using the five sets of point measurements, the pooled standard deviation of the shear-strength values was about 50%, which emphasizes that a single measurement cannot adequately describe the mean value.

Similar plots can be constructed for the other cases, and also for other snow properties. These also vary spatially; for example, the pooled standard deviation of the slab-depth measurements across slopes was about 24%, and this would result in variations of the applied gravitational stress.

Calculations of safety margins

From Equation (5) the safety margin of a "point" area of size A_0 is:

$$SM_{g0} = [F_S/A_0 + (\rho g h \sin\theta)_0] - (\rho g h \sin\theta)_0. \quad (14)$$

The subscript $_0$ denotes point measurements, F_S is the extra load required to shear a column of area A_0. When F_S was less than zero (the column fractured without additional force) or was greater than our physical limits, the first expression in Equation (14) (basal shear strength) was estimated using the statistical procedure described above. The second term is the gravitational driving force, and calculations of the safety margins in this manner effectively account for the influence of density, depth, and bed-surface angle, as well as basal shear strength. Figure 2 shows a plot of point values for each case. Negative values of the safety margin indicate areas of basal deficit, while positive values indicate areas of basal pinning.

Point values of the safety margin can be averaged over increasing lengths to generate a family of functions, each with a reduced standard deviation. Again, we use case 2 as an example and show mean values and standard deviations of averaged safety margins in Table I. These values were calculated considering loading from gravity alone, and point measurements were spaced 0.89 m apart.

Calculations of the standard normal variate and the variance ratio (from Equation (1)) were made for each function, and the analytical model (Equation (2)) was fitted to the variance ratio. For this case, a scale of fluctuation of 1.2 m provided the best fit to measured values, indicating that adjacent safety-margin values do show some correlation. These values are also shown in Table I.

https://doi.org/10.3189/S0022143000032196 Published online by Cambridge University Press

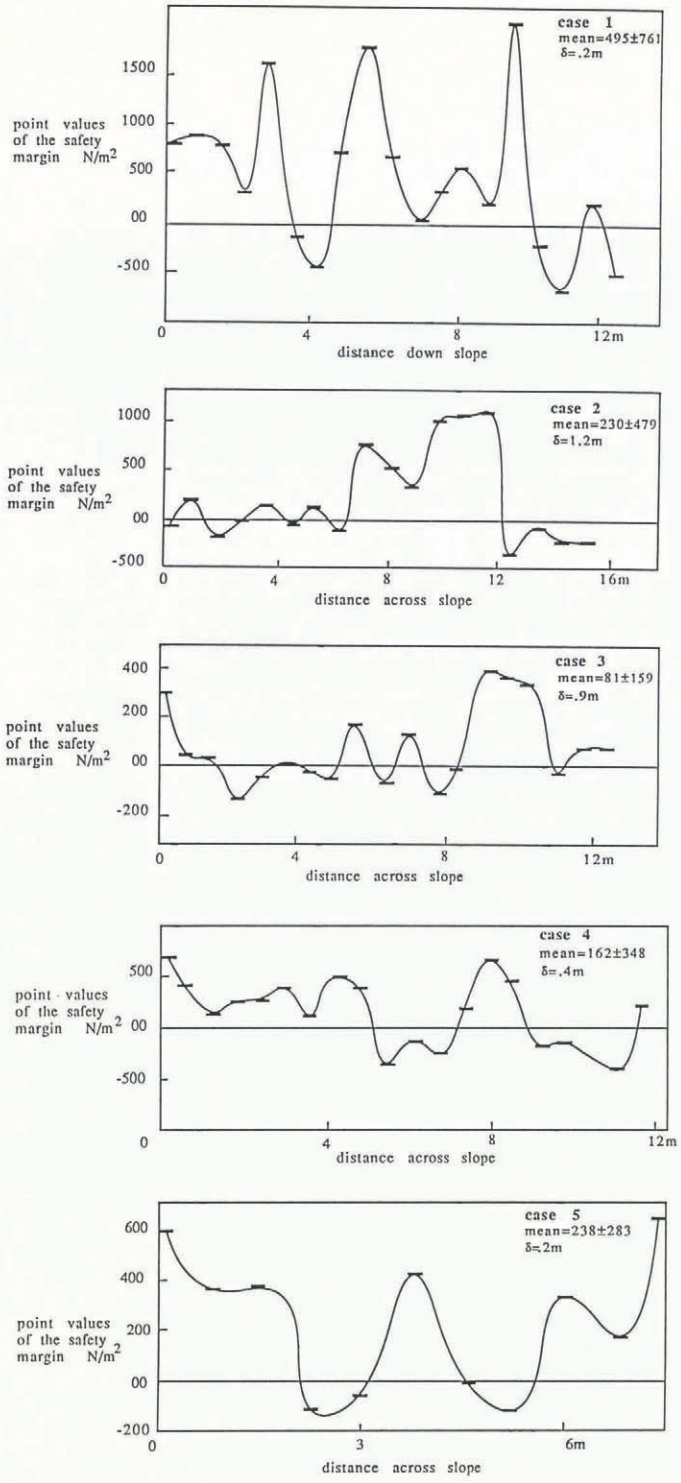

Fig. 2. For each case, point values of the safety margins have been plotted across or down slopes. These safety-margin values have been calculated from the difference between the basal shear stress and the gravitational load. A basal deficit exists when the safety margin is negative, and basal pinning occurs when the safety margin is positive. Additional loading from a skier will decrease the safety margin from those shown.

Probability of a deficit over a slope

The standard variates in Table I define the probability of a local deficit. To extend the analysis to the whole slope, we have assumed that the scale of fluctuation down-slope was the same as that across-slope, and that the length and width of deficit areas are equal. For three of the five sets of measurements, the safety margin fluctuated rapidly over short distances and the scale of fluctuation was shorter than the sampling interval. This means that adjacent values were essentially uncorrelated and can be considered to be statistically independent (cases 1, 4, and 5). In these cases, Equation (9) has been used to determine probability values for deficits of increasing areas and these are shown in Table II (the length dimension is shown for convenience). Measurements from cases 2 and 3 did show some correlation and Equation (13) has been used to determine the probabilities (also shown in Table II).

Although the probability of a local deficit may be small, if the slope size is large, the probability of one such deficit may be high. This is especially true in case 1 where the probability of a local deficit 2.8 m long was only 2×10^{-3}, but the probability of the deficit existing somewhere over the slope (area = 1.2×10^4 m^2) was 0.96. Table II shows that, as the size of deficit is increased, the probability diminishes. We have chosen 95% probability as a suitable risk of a large deficit occurring and define this as the "likely deficit length". This does not preclude a deficit of larger length which could occur either by clumping described above or because the 95% probability level is arbitary and may be too high.

The probabilities shown in the second column of Table II have been calculated considering gravitational loading only and so represent the probability of a deficit occurring naturally. The likely length differed for each slope: 2.9 m (case 1), 6.2 m (case 2), 2.7 m (case 3), 2.6 m (case 4), and about 2.0 m (case 5). Of the five cases, only case 1 had avalanched naturally. The other cases are considered below, but these measurements suggest that a likely deficit 2.9 m long was sufficient for avalanching in case 1, while likely deficit lengths less than 2.7 m were not sufficient to cause avalanches in cases 3, 4, and 5. Case 2, with a much longer (gravitational) likely deficit, does not fit this pattern, and using these arguments should have avalanched naturally. It is interesting to note that for case 2, if adjacent areas were assumed independent, the likely length was 4.2 m rather than 6.2 m, which indicates that neglecting to account for the correlation underestimates the size of the basal deficit.

Extra loading from a skier

In three of the cases we ski-released the avalanches from near the crown region. Although it is likely that dynamic loading would affect failure mechanisms, we consider only static effects by assuming that a skier jumping would shock-load an area by about four times his body weight. The extra load was taken to be 280 kg distributed along a minimum of 2 m (a typical length of ski). When considering areas less than 2 m square, we have taken the load per unit area to be proportionally less, and for larger areas the load was taken to be evenly distributed over that area. Extra loading may contribute significantly to the driving-stress term, especially when the slab is low-density and/or shallow. This reduces the safety margin and small or negative values imply that a local deficit is likely at all locations over the slope.

The three avalanches which were artificially triggered (cases 2, 3, and 4) were released by a skier at a random location on the slope (near the crownwall zone); he did not ski the entire slope but effectively loaded just one component. Case 5 was also subjected to similar skier loading but did not avalanche. The total probability of a deficit in these cases is therefore the sum of the probability of the local deficit induced by the skier, plus the probability evaluated for the unloaded section of slope. For stability estimates in other situations, the length of path taken by a skier, and the number of skiers would need to be considered in order to determine the number of components affected by extra loading.

These probabilities are listed in the third column of Table II, and comparison with the probabilities in the second column shows that skier loading increased the likely (0.95 probability) length of deficit from 6.2 m to about 6.8 m (case 2); 2.7 m to about 7 m (case 3); 2.6 m to about 4 m (case 4); and 2 m to just greater than 3 m (case 5). These results suggest that for these cases avalanching occurred if the likely length of deficit was just greater than 3 m.

As previously mentioned, if the probability of a local deficit is high, then such areas are likely to cluster to form

https://doi.org/10.3189/S0022143000032196 Published online by Cambridge University Press

TABLE. I. VALUES OF THE SAFETY MARGIN (CALCULATED FOR CASE 2 WITH GRAVITATIONAL LOADING ONLY) ARE SHOWN AS AN EXAMPLE OF THE AVERAGING PROCEDURE. POINT VALUES HAVE BEEN AVERAGED OVER INCREASING LENGTHS TO GENERATE A FAMILY OF FUNCTIONS, EACH WITH A REDUCED STANDARD DEVIATION. A STANDARD NORMAL VARIATE HAS BEEN CALCULATED FOR EACH FUNCTION, AND THE RATIO OF THE VARIANCE OF THE AVERAGED FUNCTION TO THE VARIANCE OF THE POINT FUNCTION IS ALSO SHOWN. THE VARIANCE FUNCTION CAN BE APPROXIMATED BY AN ANALYTICAL MODEL (EQUATION (2)) AND PROVIDED THE BEST FIT WHEN δ = 1.2 m

Averaging length	*Mean safety margin*	*Standard deviation*	*Standard variate*	*Variance ratio*	*Analytical model of* Γ^2
L	SM_g	SM_g	Bg	Γ^2	(δ = 1.2 m)
m					
0	230	479	0.48	1.0	1.0
0.89	255	418	0.61	0.76	1.0
1.78	273	380	0.72	0.63	0.67
3.56	327	286	1.14	0.36	0.34
5.34	355	252	1.41	0.28	0.22
7.12	361	151	2.38	0.10	0.17

TABLE II. PROBABILITIES THAT A DEFICIT WILL EXIST SOMEWHERE OVER THE SLOPE ARE SHOWN FOR DEFICITS OF INCREASING AREA (WE SHOW THE LENGTH DIMENSION FOR CONVENIENCE). THE PROBABILITIES IN THE SECOND COLUMN HAVE BEEN DETERMINED CONSIDERING GRAVITATIONAL LOADING ONLY, WHILE THE PROBABILITIES IN THE THIRD COLUMN ALLOW FOR SKIER LOADING. FOR EACH CASE, THE SLOPE AREA A_t AND THE SCALE OF FLUCTUATION δ IS ALSO SHOWN. THE CALCULATIONS WERE MADE ASSUMING THE LENGTH AND WIDTH OF DEFICIT ZONES ARE EQUAL AND, WHERE δ WAS SHORTER THAN THE SAMPLING INTERVAL, MEASUREMENTS WERE TAKEN TO BE STATISTICALLY INDEPENDENT. OF THESE, CASE 1 AVALANCHED NATURALLY; CASES 2, 3, AND 4 AVALANCHED WITH EXTRA LOADING FROM A SKIER, AND CASE 5 FRACTURED LOCALLY BUT DID NOT AVALANCHE AFTER SKIER LOADING

	Length of deficit	*Probability of deficit over the slope (gravity load)*	*Probability of deficit over the slope (plus extra load)*
	L		
	m		
Case 1	2.1	1.0	
A_t = 1.2 × 10^4 m^2	2.8	0.96	
δ = 0.2 m	4.2	0.18	
λ = 0.5 m			
Case 2	5.34	1.0	1.0
A_t = 600 m^2	6.23	0.95	1.0
δ = 1.2 m	7.12	0.68	0.70
λ = 3.0 m	8.01	0.22	0.22
Case 3	2.1	0.97	1.0
A_t = 90 m^2	3.5	0.90	1.0
δ = 0.9 m	5.6	0.77	1.0
λ = 2.25 m	7.0	0.65	0.96
Case 4	2.4	0.98	1.0
A_t = 120 m^2	3.0	0.80	1.0
δ = 0.4 m	3.6	0.52	1.0
λ = 1 m	4.2	0.45	0.81
	5.4	0.31	0.56
Case 5	1.5	1.0	1.0
A_t = 108 m^2	2.25	0.82	1.0
δ = 0.2 m	3.0	0.20	1.0
λ = 0.5 m	3.75	0.19	0.62
	4.5	0.02	0.17
	5.25	$<10^{-4}$	2 × 10^{-4}

https://doi.org/10.3189/S0022143000032196 Published online by Cambridge University Press

a deficit area which would be larger than that predicted by theory. This condition is especially likely in the cases which were loaded by a skier.

DISCUSSION AND IMPLICATIONS FOR STABILITY ASSESSMENT

Sampling errors

It is possible that our measurements around the peripheries of avalanched slopes do not adequately represent the strength values (and the variability) for the entire slab, and our method of testing may induce a bending moment at the shear layer. Furthermore, the measurements were done with rates, size of sample, etc., which were convenient, and not necessarily those applicable to the particular avalanche. We hoped to keep the measurements self-consistent by making measurements over 0–5 s for failure, but snow-strength properties vary significantly with strain history and strain-rates. We are uncertain of the magnitude of this influence which is likely to provide a relatively constant error and for these reasons the strength measurements should be considered as an index only.

We suspect that the error in measuring the force required to shear a column and measuring the area of the shear plane each to be about 10%. This would result in a total measuring error of about 14%, which would fluctuate over short scales (between measurements). The pooled standard deviation of our estimates of point values of safety margin was about 170%, and in some cases the standard deviation from the mean was greater than 200%. Although both the magnitude and the correlation scale of this error would be contained in our estimate of the statistical parameters of the safety margins, we expect their influence to be small.

Optimum sampling interval and number of measurements

In an earlier paper we suggested that spatial variations of strength might originate from local air-flow patterns occurring at the time of deposition of the snow layer (Conway and Abrahamson, 1984). Potential avalanche slopes are commonly those lee to a prevailing wind, and above such slopes there is considerable turbulence. The nature of the turbulence commonly results in complex patterns of ripple forms on the snow surface with a variety of spacings and orientations. We have measured the wavelength of surface snow waves in the range from 10 mm to 15 m (and commonly less than 5 m). We suspect that, when such ripples are buried by subsequent snowfalls, the pattern may be preserved and reflected in the wavelength of the strength values. Somewhat different are the large dunes or drifts of snow which commonly form behind discontinuities in terrain. These are likely to cause changes in both the mean strength and the load.

Equation (3) can be used to calculate an approximate wavelength for each of the sets of measurements of shear strength and these suggest that the five sets of measurements fluctuated with relatively short wavelengths (λ was always less than 3.25 m). We are uncertain whether this short-scale fluctuation pattern is typical, but note that Sommerfeld (paper in preparation) also found variations over short distances (e.g. three-fold variation in measurements made over 5 m). The wavelength of shear-strength measurements down-slope (case 1) did not differ significantly from those measured across slopes. Although we acknowledge that the pattern may vary depending on the orientation and spacing of the ripples or dunes (which in turn depend on the local wind direction), we have assumed for a first approximation that the strength distribution down-slope is similar to that across-slope.

The pooled standard deviation of our measurements of slab depth (about 24%) was less than that of the shear-strength measurements (about 50%), and correlation scales of the depth measurements were longer (δ varied from 0.5 to 2.3 m) than those of the strength measurements (0.2–1.3 m). This is expected since slabs generally consist of several deposits of snow which would tend to average the fluctuations from each layer. The standard deviation and correlation scale of the safety-margin values contain information about variations in both the depth and shear strength, and these suggest that the safety margin also fluctuated over short distances (wavelength less than about 3 m; see Table II).

To estimate the mean, standard deviation, and correlation structure of a function, the optimum sampling interval needs to be about one-half the wavelength and made over at least one wavelength. If one could be certain that the mean safety margin was not changing across a slope and, if the observed pattern of short-scaled fluctuations is typical, these parameters could be estimated with a few closely spaced measurements (0.5 m) over at least 3 m. However, especially over large slopes, a more slowly varying trend in strength or loading may exist superimposed on the pattern of rapid fluctuations. For an adequate estimate, these cases would require several sets of contiguous measurements at intervals of one-half the scale associated with the slowly varying trend. In fact, in case 2, the mean safety margin changed by about 60% with spatial averaging which suggests the data were not strictly homogeneous (on the scale of our measurements), and the mean changed across the slope. In this case, several closely spaced measurements at only one location might have resulted in an unreasonably high (or low) estimate of the safety margin.

Size of deficit zones and failure models

Size of deficit zones

We acknowledge there are likely to be many factors besides the size of basal deficit which will affect the stability of a slope. Some of these, such as stress–strain properties and history, and dynamic effects, have been mentioned briefly. Also of importance may be the contribution from within the slab in resisting the loading forces. For instance, the tensile stresses required to fracture (or initiate fracture) of a deep, high-density slab are likely to be higher than for a shallow, low-density slab. The critical area of deficit is therefore likely to be different for each case, and our calculations do not account for any of these factors. We have considered only the area of deficit as a criterion for stability.

In some cases, the probability of occurrence of a deficit decreased rapidly as the size of deficit was increased. For example in case 1, the probability of finding a deficit of the same size as the avalanche (1.2×10^4 m^2) was extremely small ($<<10^{-4}$), and the most likely deficit area was only 2.9 m square or about 8.5 m^2. This suggests that the fracture initiated from a small local deficit which enlarged to cause the avalanche. It should be noted that this was the only case where more than a couple of hours had elapsed between avalanching and testing, and it is possible that the snow may have strengthened during this interval (12 h).

The other avalanches were smaller and triggered by skier loading which effectively increased the size of the basal deficit (loading increased the 95% deficit area by over 600% in case 3). These areas were always less than 7 m square (49 m^2), but Table II shows that there is also a finite probability that a deficit could have existed over larger areas; for example, in case 2 skier loading could be expected to produce a deficit of about 64 m^2 (22% probability), and in case 4, a deficit of about 30 m^2 (56% probability). Although these areas represent a large proportion of the respective slopes, they are small when compared with many avalanche slopes and we suspect that, in general, avalanches may be triggered by relatively small areas of deficit (length less than 7 m and even as small as 2.9 m). These small deficits would then enlarge by some mechanism to cause an avalanche. It would be useful to make further measurements to confirm whether this length is typical, and it is important to remember that with the number of tests being limited practically by time, it will be uncommon to find a deficit which spans as far as the length calculated.

Although case 5 did not avalanche, it was very unstable. Table II shows that one of the main differences between this case and the others which did avalanche after skier loading was that the probability of a deficit over larger areas was very small (e.g. for a deficit 5.25 m long, the probability was 2×10^{-4}). This, combined with hold-up from the slab or some other mechanism, may have inhibited avalanching.

https://doi.org/10.3189/S0022143000032196 Published online by Cambridge University Press

Comparison with failure models

Several models of slope failure have been proposed and most require a basal deficit to exist over some length. One simple model proposed by Perla and LaChapelle (1970) requires that the loss in shear support over half the length of a deficit zone is taken up in the tensile region. The deficit is pinned at each end and cannot enlarge. If the deficit is large and exists over a sufficiently long length, the induced stresses may exceed the tensile strength of the slab, resulting in a tensile failure. (For details of the model, see Perla and LaChapelle, 1970.) Although this model does not strictly represent conditions expected within a slab, it could be expected to provide an order-of-magnitude estimate of the length of deficit required to fracture a slab of particular depth and tensile strength. Using estimates for the tensile strength and Poisson's ratio of the slab, for the above cases these lengths varied from 2.2 to 7 m (before additional loading). These lengths are of the same order as those found in our probability analysis.

In many cases, it is unreasonable to expect the size of the deficit zone to be fixed, and Palmer and Rice (1973) proposed a model for soil slopes which described the expansion of a basal shear deficit. The model requires the material in the basal zone to weaken or "shear-strain soften" after a slip displacement. A deficit would result in strain energy being stored in the slab, and propagation would occur if this energy was in excess of that required to expand the flaw by further strain-softening. This has been applied to snow by McClung (1979, 1981), although he did not consider how the mechanism might initiate and he considered the case where the shear strength dropped from constant peak to residual values. Recently, Abrahamson and Conway (paper in preparation) used the J integral method proposed by Palmer and Rice to allow for variations of basal shear strength. They considered an area of basal deficit which was surrounded by a zone of higher strength, and calculated the minimum length of deficit which could provide sufficient energy to allow expansion through the pinned area. (For details of the models see Palmer and Rice, 1973; McClung, 1979, 1981; Abrahamson and Conway, paper in preparation.) It is unlikely that this model will represent conditions exactly either, but we have inserted typical values of snow properties in the Abrahamson and Conway adaptation, and calculated the minimum lengths required for expansion of a deficit. For the above cases, these lengths ranged from about 1.8 to 7.2 m before additional loading, which further supports the idea that avalanches initiate from small zones of deficit.

CONCLUSIONS

Stresses in regions surrounding a basal shear deficit will increase especially if the deficit exists over a large area. If the stresses become sufficiently large, they will cause either a local failure or expansion of the deficit and either of these mechanisms is likely to initiate avalanching. By comparing applied static loads and basal shear strengths from areas beside avalanches, it was found that slopes typically contained areas of basal shear deficit and areas of basal shear excess (pinned areas) A primary consideration for slope stability is the pattern of the deficit and pinned areas, and statistical theories have been used to describe the variations of strength and stress measured across avalanche slopes.

Measurements made over slopes were used to determine a probability distribution for the length of deficit. Several of the avalanches were triggered by a skier, and this effect was approximated by considering the extra static loading expected from a skier. Extra weight increases both the magnitude and the length of a deficit, and would be particularly significant when the slab was shallow and/or of low density. In this study, slopes which had avalanched were estimated to have contained a deficit which spanned over at least 2.9 m (95% confidence). For slopes which had not avalanched, the expected length of deficit was usually shorter than 2.9 m. These lengths are small compared with the size of typical avalanche slopes. It should be noted that most of the measurements were made around relatively small avalanches, and it would be important to determine whether this pattern is also typical on larger slopes.

Also calculated for each slope studied were the lengths of basal shear deficit required to cause (a) tensile fracture of the slab; (b) expansion of the deficit through surrounding pinning areas. The lengths required for instability by these models were of the same order as the likely lengths (0.95 probability) calculated from our shear measurements. This strongly suggests that the avalanches in this study initiated from relatively small zones of deficit, and this may be a general feature of slab avalanches.

The wavelength of the variations of the safety margin was less than 3 m, and adjacent measurements commonly differed in magnitude by about 200%. In these cases, a single random test would not adequately describe the safety margin over the entire slope and a primary concern for stability assessment is to evaluate the variance and statistical correlations, as well as the mean value. If the pattern we have observed is typical, then a reasonable estimate may be possible only with several closely spaced tests (sample interval of about 0.5 m, and tests spanning at least 3 m). A rapid test for obtaining a quantitative measure of shear deficit over such a distance has been proposed recently by Conway and others (1986).

ACKNOWLEDGEMENTS

The Department of Lands and Survey (Wellington, New Zealand) and the University of Canterbury (Christchurch, New Zealand) provided financial support for the study. Mount Cook Airlines provided transport to the field area, and assistance from Mount Cook National Park staff was invaluable. We are grateful to all these people for their assistance.

REFERENCES

Conway, H., *and* Abrahamson, J. 1984. Snow stability index. *Journal of Glaciology*, **30**(106), 321-27.

Conway, H., Abrahamson, J., *and* Young, R. 1986. A field test to assess snow-slope stability. *Journal of Glaciology*, **32**(112), 535-37.

Crandall, S.H., Chandiranani, K.L., *and* Cook, R.G. 1966. Some first passage problems in random vibration. *Journal of Applied Mechanics*, Ser. E, **33**, 532-38.

Gubler, H. 1978. An alternate statistical interpretation of the strength of snow. *Journal of Glaciology*, **20**(83), 343-57.

Harr, M.E. 1977. *Mechanics of particulate media.* New York, McGraw-Hill.

Krige, D.G. 1966. Two dimensional weighted moving averaging trend surfaces for ore evaluation. *In Symposium on Mathematical Statistics and Computer Applications for Ore Evaluation, Johannesburg, South Africa. Proceedings*, 13-38.

McClung, D.M. 1979. Shear fracture precipitated by strain softening as a mechanism of dry slab avalanche release. *Journal of Geophysical Research*, **84**(B7), 3519-26.

McClung, D.M. 1981. Fracture mechanical models of dry slab avalanche release. *Journal of Geophysical Research*, **86**(B11), 10783-90.

Nguyen, V.U., *and* Chowdhury, R.N. 1985. Simulation of risk analysis. *Géotechnique*, **35**(1), 47-58.

Palmer, A.C., *and* Rice, J.R. 1973. The growth of slip surfaces in the progressive failure of over-consolidated clay. *Proceedings of the Royal Society of London*, Ser. A, **332**, 527-48.

Perla, R.I., *and* LaChapelle, E.R. 1970. A theory of snow slab failure. *Journal of Geophysical Research*, **75**(36), 7619-27.

Rice, S.O. 1944. Mathematical analysis of random noise. *Bell System Technical Journal*, **23**, 282-323; **24**, 46-156.

Sarhan, A.E., *and* Greenberg, B.G., *eds. Contributions to order statistics*. New York, Wiley and Sons.

Vanmarcke, E.H. 1975. On the distribution of the first-passage time for normal stationary random processes. *Journal of Applied Mechanics*, Ser. E, **42**, 215-20.

Vanmarcke, E.H. 1977[a]. Probabilistic modeling of soil profiles. *Journal of Geotechnical Engineering*, **GT103**(11), 1227-46.

https://doi.org/10.3189/S0022143000032196 Published online by Cambridge University Press

Vanmarcke, E.H. 1977[b]. Reliability of earth slopes. *Journal of Geotechnical Engineering*, **GT103**(11), 1247-65.
Vanmarcke, E.H. 1983. *Random fields, analysis and synthesis*. Cambridge, MA, MIT Press.

APPENDIX

SUMMARY OF STRENGTH MEASUREMENTS

Case 1. 19 September 1982, cornicewall: 19 shear-strength measurements (five fractured before the extra load was applied, or "fell out") down the flankwall of an avalanche that had released naturally about 15–24 h previously. The avalanche released naturally and followed a period of considerable snowfall and wind transport of snow (new snow depths of 1–2 m were measured), and this deposit overlay about 1 mm in diameter faceted crystals which formed a layer up to 40 mm thick. The avalanche was about 150 m wide and 80 m long.

Case 2. 13 July 1982, cornicewall: 18 shear-strength measurements (nine fell out) across the crownwall of an avalanche that had been ski-released. Three tensile-strength measurements were also made. This was a medium–soft slab and the shear layer consisted of new snow including capped columns, columns, stellars, needles, and plate crystals which were less than 1 mm in diameter and partly rimed. The fracture occurred within the new snow (no discontinuity was observed). Ski-loading near the crown had caused local failure of a section about 4 m^2 in area, which slid about 0.7 m before the rest of the slab fractured. The avalanche was about 30 m wide and 20 m long.

Case 3. 1 August 1984, cornicewall: 19 shear-strength measurements (nine fell out) across-slope This small avalanche (12.5 m wide and 7 m long) was ski-released from near the middle of the crownwall. The slab consisted of rounded, wind-affected, partly metamorphosed crystals. The slab sheared on some very soft snow (1 mm in diameter partly rimed capped columns, columns, dendrites, and needles).

Case 4. 28 August 1984, cornicewall: 20 shear-strength measurements (seven fell out) made across-slope. This small avalanche (12 m × 10 m) required ski-loading for release. The slope had been wind-loaded with heavily rimed and rounded snow crystals, and the slab slid at the upper boundary of a layer of soft low-density snow which also contained some 1 mm diameter faceted crystals. After making measurements across the fracture, a further section of the slope (about 5 m further north) was released by skiing.

Case 5. 10 August 1983, cornicewall: 11 shear-strength measurements (five fell out) across the slope. Extensive jumping on the slope resulted in local failures and slabs about 2 m square slid a short distance. The fractures did not enlarge to cause an avalanche, but the potential avalanche area was about 12 m × 9 m. The shear layer was 40–50 mm thick and consisted of 0.5–1.5 mm diameter graupel at a temperature of −5.0 °C.

Particular details for each case are listed below:

	Case 1	*Case 2*	*Case 3*	*Case 4*	*Case 5*
Spacing between measurements (m)	0.7	0.89	0.7	0.6	0.75
Bed-surface angle	34°	47°	35–56°	45–49°	35–50°
Slab density (kg/m^3)	290	140	180	260	280
Slab depth (m)	0.93 ± 0.1	0.43 ± 0.09	0.18 ± 0.03	0.25 ± 0.08	0.43 ± 0.16
Mean point SM_{go}	495 ± 761	230 ± 479	81 ± 159	162 ± 348	238 ± 283

MS. received 19 January 1987 and in revised form 27 January 1988

https://doi.org/10.3189/S0022143000032196 Published online by Cambridge University Press